Patch clamp recordings from membranes which contain gap junction channels

Peter R. Brink and Shih-fang Fan
Department of Anatomical Sciences, Health Science Center, School of Medicine, State University of New York at Stony Brook, Stony Brook, New York 11794

ABSTRACT The septal membranes of the median and lateral giant axons of earthworm, which contain gap junctions, were exposed by cutting one segment of the cord. Patch recordings were obtained from the exposed cytoplasmic side of the septum. Seal resistances ranged from 2 to 15 GΩ. The patch could be excised (detached) or left attached to the whole cell. Two types of channels were observed. One type was blocked by tetraethylammonium (TEA) or Cs^+ and had a unitary conductance of 30–40 pS. It appears to be a K^+ channel. The other channel type had a unitary conductance of 90–110 pS and was unaffected by TEA^+ or Cs^+. In the detached configuration the channel was shown to conduct Cs^+, K^+, Na^+, TMA^+, Cl^- and TEA^+ even in the presence of 2 mM Zn^{2+}, 1 mM Ni^{2+}, 1 mM Co^{2+}, and 4 mM 4-aminopyridine. The conductance ratios relative to K^+ were 1.0 for Cs^+, 0.84 for Na^+, 0.64 for TMA^+, 0.52 for Cl^- and 0.2 for TEA^+. The channel appears to be voltage insensitive whether monitored in detached or attached recording mode. Both H^+ and Ca^{2+} reduce the probability of opening. Thus, the 100 pS channel has many of the properties expected of a gap junction channel.

INTRODUCTION

The gap junction channel links the cytosols of two adjacent cells. It is composed of 12 subunits (Goodenough, 1975). Six subunits assembled in the plasma membrane of one cell form the potentially conductive membrane protein channel referred to as a hemichannel. Two such units form an intercellular channel or gap junction channel. Gap junctional membrane conductance has been shown to be regulated by H^+ (Spray et al., 1984). In addition Ca^{2+} (Loewenstein, 1981), transjunctional potential in a number of preparations (Spray et al., 1984), and plasma membrane potential in salivary gland cells of larval forms of *Drosophila* (Verselis et al., 1988) and *Chironomus* (Obaid et al., 1983) have been shown to alter the coupling coefficient or junctional conductance. Other investigators have observed gap junction channel activity using double whole cell patch clamp methods. In the double patch mode channel openings of equal but opposite sign seen simultaneously on the two current traces indicate a gap junction channel opening between the two patched cells (Veenstra and DeHaan, 1986). In neonatal chick and rat cardiac cell pairs Veenstra and DeHaan (1986) and Burt and Spray (1988) have demonstrated 120–160 pS and 50 pS channels, respectively. Neyton and Trautmann (1985) double patched rat lacrimal gland cell pairs and reported the occurrence of 120 pS channels and determined their selectivity to Na^+ and Cl^- relative to K^+.

The double patch method has two requirements: high cell input impedance (1 GΩ or more) and a low number of gap junction channels connecting the two patched cells. If the number of channels is too great or the cell impedance is too low discrete channel activity is not resolvable in the current noise in either patch. In the case of neonatal chick cells these requirements are met (Veenstra and DeHaan, 1986), but the method can not be used to monitor single gap junctional membrane channels in adult myocytes, where the junctional membrane conductance can be 1 μS (Weingart, 1986).

In two studies reconstitution into bilayers has been employed. Hall and Zampighi (1985) reconstituted the MIP26 from lens. It is not yet clear whether MIP26 is indeed a subunit of the gap junction. Nonetheless, the single channel conductance was 200 pS in 100 mM KCl at pH = 5.7. Four distinct conductive states were observed: 50, 100, 150, and 200 pS. Because the subunits were reconstituted into a lipid bilayer the observed activity could be the result of opening the hemichannels. A similar study was performed by Ding-E Young et al. (1987) with the rat liver 27 KD subunit. They reported a single channel conductance of 140–270 pS with a salt concentration of ~ 100 mM and 1 mM Ca^{2+}. The incorporated protein channels from liver and lens showed some voltage dependence. In another study whole junctional membrane fragments from rat liver were reconstituted into a lipid bilayer (Spray et al., 1986). The observed single channel conductance was 100 pS in 150 mM salt solution. Application of antibodies raised against rat liver gap junctions resulted in the loss of channel activity.

We have taken a different approach in an attempt to

0006-3495/89/09/579/15 $2.00

directly observe gap junction channel activity in a fully differentiated cell pair. In this case the cytoplasmic side of one cell connected to another via gap junctions is exposed and a patch electrode introduced onto the surface of the gap junction-containing membrane. Because it is difficult to verify what is within the tip of the patch electrode or truly on the denuded cytoplasmic surface of the ruptured cell we have used a number of criteria to help in determining whether observed channels are gap junction-like. The following criteria were used: (*a*) whether the channels found in on-cell patches were in electrical contact with the adjacent intact cell; (*b*) cation selectivity (conductance ratios); (*c*) anion permeability, for example the ability of the channel to pass Cl^-; (*d*) H^+ and Ca^{2+} sensitivity; (*e*) the effects, if any, of channel blocking agents such as tetraethylammonium (TEA^+), Cs^+, Zn^{2+}, Ni^{2+}, 4-aminopyridine and Co^{2+} and (*f*) voltage dependence in cell attached and detached recording modes.

The preparations used are the septate median and lateral giant axons of the earthworm. Each neuron within a segment contains an axon that is ~ 1 mm in length and 60–100 μm in diameter. The interface between two axonal segments is comprised of the two apposed membranes of two adjacent axon segments and is defined as a septum (Stough, 1930). Gap junctions in the septal membrane form the connecting pathway between two abutting segmental axons (Kensler et al., 1979; Brink and Dewey, 1978). Macroscopic measurements of junctional membrane conductance using double voltage clamp and single internal ground voltage clamp have shown that the conductance of the junctions of the septal membranes are sensitive to neither transjunctional potential nor to plasma membrane potential over a large potential range (Brink et al., 1988). The conductance of the junctional membrane is sensitive to pH (Verselis and Brink, 1984). The pH sensitivity is much like that of adult heart myocytes (White et al., 1985).

METHODS

Earthworms were maintained at 5°C as previously described (Brink and Barr, 1977). Ventral nerve cords containing median and lateral giant septate axons were dissected in saline which contained 150 mM NaCl, 2 mM $CaCl_2$, 1 mM $MgCl_2$, 1 mM KCl, and 10 mM Hepes, pH = 7.35. The cords were pinned out on a Sylgard-coated dish (5 ml) and cut perpendicular to the long axis of the cord at points where nerve branches arise positions where septal membranes often occur (Fig. 1). Once the cuts were made the 1–2 mm long segments were allowed to stand in saline for 10–20 min. This procedure is similar to that used by Benzanilla (1987). Presumably the 2 mM Ca^{2+} activates cytoplasmic proteases that in turn partially denudes the cytoplasmic surface of the junctional membrane. After the 10–20 min 2 mM Ca^{2+} exposure the preparations were perfused with KCl or CsCl saline (Table 1). All salines used for patch clamp experiments contained TEA^+, Co^{2+}, Zn^{2+}, and Ni^{2+}. The calculated free Ca^{2+} was 10 nm (pCa = 8, Nanninga and Kemper 1971) in all salines used for patch recordings, the exception being CsCl-Ca saline where the Ca^{2+} concentration was 2 mM. Patch pipettes with an outside tip diameter of 1–2 μm were filled with solution identical to the perfusate. Junction potentials in all but the low ionic strength salines were +1 mv (KCl solution vs. CsCl solution), −1 mv (KCl solution vs. NaCl solution), −1.7 mv (KCl solution vs. TMACl solution), and − 3 mv (CsCl solution vs. TEACl solution). With low ionic strength salines an agar reference electrode was used which contained the same media as the patch pipette. The measured junction potential was −2 mv using an agar bridge for low chloride solutions. In all cases the junction potentials were subtracted from the apparent reversal potentials to yield the values given in Table 2.

All solutions were filtered with 0.22 μm (Millipore Corp., Bedford, MA). Seals were obtained by bringing the patch pipette into contact with the exposed membrane. Application of a negative pressure produced seals in the 2–15 GΩ range. In early experiments, when the preparation was perfused with saline containing KCl but no TEA^+ a 30–40 pS K^+ channel was observed. Both Cs^+ and TEA^+ successfully blocked this channel, confirming it as a K^+ channel and in subsequent

TABLE 1 Saline type

	KCl	CsCl	NaCl	TMA	TEA	$CsCl_{low}$	KCl_{low}	CsCl-Ca
Salt								
KCl	135	1	1	1	1	1	55	1
CsCl	1	135	1	1	1	30	1	135
NaCl	1	1	135	1	1	1	1	1
TMACl	1	1	1	135	1	1	1	1
TEACl	30/10*	30/10*	30	30	135	10*	10*	30
$ZnCl_2$	2	2	2	2	2	2	2	2
$CoCl_2$	1	1	1	1	1	1	1	1
$NiCl_2$	1	1	1	1	1	1	1	1
EGTA	0.6	0.6	0.6	0.6	0.6	0.6	0.6	0
$CaCl_2$	0.1	0.1	0.1	0.1	0.1	0.1	0.1	2
Hepes	10	10	10	10	10	10	10	10
Sucrose						210	160	

*10 mM TEABr.
All values are given in millimolars.

TABLE 2

	KCl/KCl	KCl/KCl_{low}	CsCl/$CsCl_{low}$	KCl/CsCl	KCl/NaCl	KCl/TMA	CsCl/TEA
E_K	0	−22	0	−121	−121	−121	0
E_{Cs}	0	0	−37	+121	0	0	−121
E_{Na}	0	0	0	0	+121	0	0
E_{Cl}	0	+22	+37	0	0	0	−4
E_{TMA}	0	0	0	0	0	+121	0
E_{TEA}	0	0	0	0	0	0	+37
E_r	0	−7	−10	0	−8	−20	−65
		$G_{Cl}/G_K = 0.52$	$G_{Cl}/G_{Cs} = 0.57$	$G_{Cs}/G_K = 1$	$G_{Na}/G_K = 0.84$	$G_{TMA}/G_K = 0.64$	$G_{TEA}/G_{Cs} = 0.2$

Conductance ratio sequence K = Cs > Na > TMA > Cl > TEA.
E_r = reversal potential, all other E values are the equilibrium potentials for the respective ions.

experiments TEA^+ and Cs^+ were present in the perfusate and patch electrode. Nonetheless, Zn^{2+} and Ni^{2+} or Co^{2+} were also added to the perfusate and patch electrode to block anion and Ca^{2+} channels. While these ions might themselves affect gating the fact that the 100 pS channel can function with these ions present indicates that it is not a Cl^- or Ca^{2+} channel for example. In a number of experiments 4-aminopyridine was also added to the patch pipette solution and bath.

Experiments were performed on both cell-attached and detached patches. In some cell-attached patches a microelectrode was inserted into the intact cell. The microelectrodes had tip diameters of 0.5 μm and were filled with 2M KCl (10 MΩ). Channel(s) were observed in the attached mode and reversal potentials determined. In cases where a microelectrode had been inserted into the intact axon 220 ms-duration depolarizing current injections were applied periodically to determine if observed channels were in electrical contact with the intact cell. Typically, microelectrodes were inserted 100 to 200 μm from the sight of patch attachment. The median and lateral axons have length constants of 2–4 mm (Brink and Barr, 1977) thus the voltage drop between the source of current injection and the sight of the attached patch was minimal, <5% decay of potential. After recording channel activity in the attached mode the patch was then detached and the shift in reversal potential was recorded. In the detached mode solutions of various compositions were perfused into the Sylgaard dish to test the Ca^{2+} and pH sensitivity of the channels as well as ion selectivity. Selectivity was tested by substitution of KCl or CsCl saline with NaCl, TMACl or TEACl salines (see Table 1 for composition of salines). Perfusion with low concentrations of KCl (55 mM) or CsCl (30 mM) with sucrose added (160 mM and 210 mM respectively), to maintain osmolarity, were used to test anion permeability relative to K^+ or Cs^{2+}. Perfusion rates were 5–15 ml/min. For the anion experiments 10 mM TEABr was used in bath and pipette solutions. A WPI (S-7050A) patch clamp amplifier was used to record channel activity. Data were collected via a Data Translation 2801 A/D board in an IBM XT formatted to include a virtual disc. 10 to 35 s records were taken at 0.5 ms or 1.75 ms sampling rates. 0.5 ms sample rate records were filtered with a low pass filter at 1 KHz and those at 1.75 ms at 0.3 KHz. The time required to store a record in the virtual disc was 0.4 s. Once the virtual disc was full (24 records) it was down-loaded to floppy discs or tape. Under any condition at least 140 s of records were obtained; the exception being the data in Fig. 3 that represents only 40 s at each sample. For every 140 s of recording 1.2 s was lost in storage time to the virtual disc (0.85%). Histograms of current distribution were generated using point by point analysis. The ground state or state of least current flow was arbitrarily set to zero. This allowed for unitary current to be determined accurately. The number of unitary events was also calculated in each case via computer by setting a discriminator midway between each level or state. Each transition from one state to another constituted an event.

RESULTS

A fluorescent micrograph of a segment of the *in situ* median axon after injection with the dye carboxyfluorescein (CFL) is shown in Fig. 1 *a*. The septa act as barriers to the diffusion of the probe. The arrows indicate the positions of the septal membranes. Analysis of the diffusion of various probes like CFL have shown the gap junctions of the median axon are permeable to probes with diameters of 1.0–1.4 nm (Brink and Ramanan, 1985). Fig. 1 *b* shows a light micrograph of the cut end of a nerve cord. A septal membrane can be seen protruding from the cut end of the cord. A dye filled microelectrode, which was inserted into the axon at the septal membrane, indicates the position of the membrane. The microelectrode was filled with fluorescein-sulfonate (Molecular Probes, Inc., Eugene OR). Hyperpolarizing current steps were applied to fill the partially dissected septate axon. Fig. 1 *c* illustrates the fluorescent image of the dye filled axon shown in Fig. 1 *b*. It indicates that the exposed septal membrane is continuous with the axonal segment. The dye fill also shows the position of the adjacent septal membrane within the nerve cord (arrow). Note that the septum extends out from the cut end of the cord. This is most likely due to contraction of smooth muscle cells within the cord. The channel activity observed was the same whether lateral or median septal membrane was patched. Because the septum was protruding the effect of stretch was also considered. We found that application of negative pressure to the pipette had no effect on channel activity in detached patch mode.

Attached patch recordings

Recordings made while the patch was attached to the septal membrane were performed under two conditions: either with a microelectrode in the intact cell or without a microelectrode. All cell-attached recordings were done

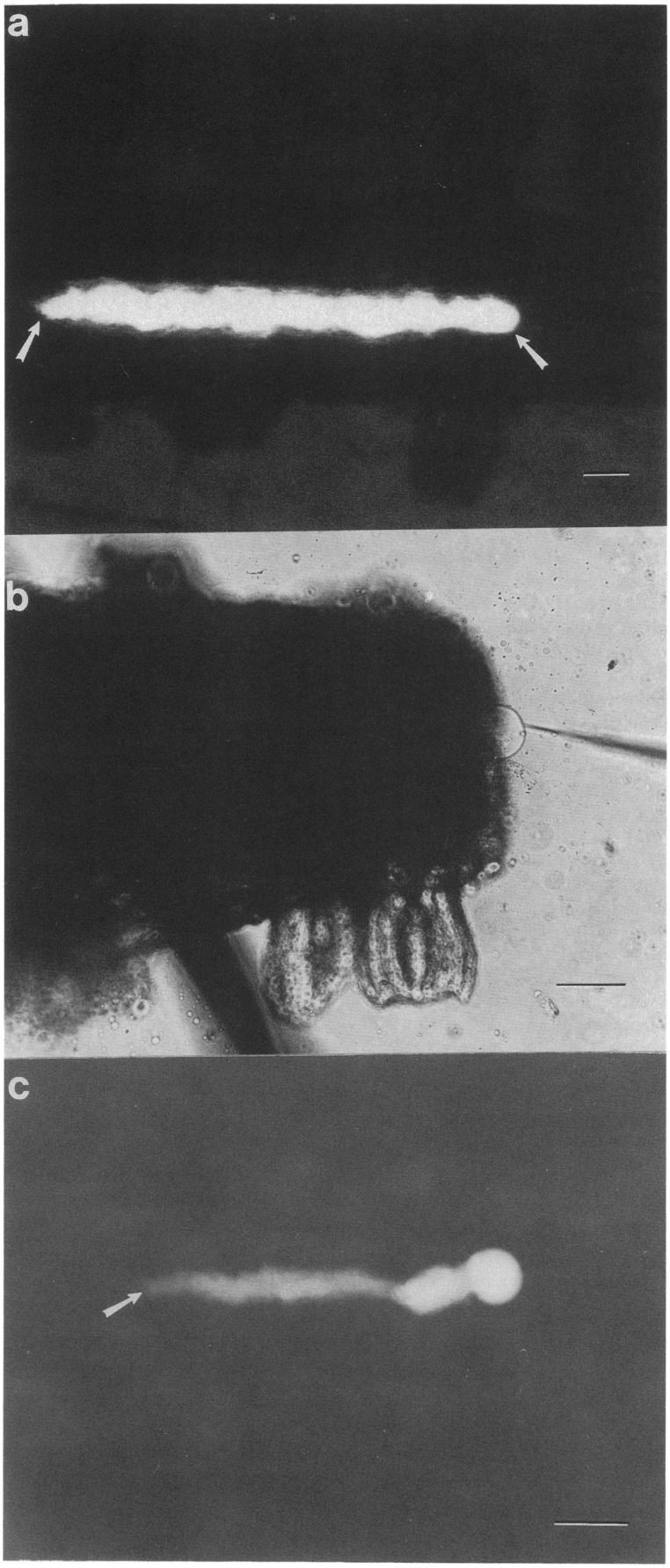
a
b
c

after the preparation had been perfused with the low Ca^{2+} perfusate (Ca^{2+} = 10 nM). The microelectrode impalements of the partially exposed axons yielded resting potentials ranging from −7 to −38 mV. The average was −17.5 mV (n = 8, SD ± 10.2 mV). The normal resting potential of the intact axon in a typical saline (NaCl = 140 mM, $CaCl_2$ = 1 mM) is −70 mV (Brink and Barr, 1977). The decrease in resting potential is very likely a result of the rigors of dissection and bathing of the exposed septal membrane in salines with low Ca^{2+} levels. Under these conditions the gap junction channels facing the bath are free to allow ion transport to and from the bath and intact cell. Because the channels are relatively nonselective, the axon resting potential is expected to depolarize as these results indicate. The depolarization of the axon will not affect the behavior of the gap junctions because under double voltage clamp membrane potential has been shown to have no effect on channel patency (Brink et al., 1988).

Fig. 2 *a* illustrates the positions of the patch electrode and the intracellular microelectrode used to deliver current pulses to the axon. Fig. 2 *b* shows the results obtained with such an experimental arrangement. Short duration current pulses were applied through the microelectrode that had been inserted into the intact cell some 150 μm away. The resting potential recorded with the microelectrode was −20 mV (V_m). The trace labeled I_e shows the applied current steps delivered through the microelectrode. 20 nA steps were applied through the intracellular microelectrode. The trace labeled I_c shows current flow through the patch electrode. The *C* and *O* designations indicate closed and open states, respectively. The Cs/Cell designation indicates that the pipette was filled with CsCl saline and was attached to the septal membrane. The perfusate was also CsCl saline with a pH = 6.8. In trace I_c (holding potential = +40 mV) when the channel was closed a deflection was seen that was presumably due to cross talk between the patch and microelectrode due to their close proximity. When the channel was open the effect of the applied current step was readily apparent. The applied voltage step from the intracellular electrode reduced the current flow through the channel when it was open. The step resulted in a depolarization of the intact cell effectively reducing the potential across the patched membrane. This shows that the channel was in electrical contact with the interior of the intact cell. The *I-V* relationship for the channel is shown in Fig. 2 *c* and indicates that the reversal potential (E_r) was shifted from −15 mV on septum, which is similar to the resting potential of the intact cell, to 0 in the detached mode. The line fits in (*c*) were derived from least squares analysis. The slope for Cs/cell was 0.91 SE = ±0.008 and 0.86 SE = ±0.03 for Cs/Cs. The dependent variable had units of pA while independent variable had units of mV. Records taken in the attached patch mode were also used to produce amplitude histograms.

Fig. 3 illustrates two amplitude histograms of current distribution generated from such an experiment where the holding potential was held at −40 and then +40 mV, the pipette contained CsCl saline. The two amplitude histograms are mirror images, with the exception of the magnitude of the unitary current, indicating that there is little or no voltage dependence. This same behavior was seen in detached patches (Fig. 6). At −40 mV the unitary current was −3.5 pA while at +40 mV it was 5 pA indicating in this attached patch that the resting potential was ~ −7 mV. Unitary conductance was not determined because intracellular Cl^- concentration was not known. The total number of unitary events at −40 mV was 81 and at +40 mV it was 94. The pH of the CsCl saline in the patch electrode was pH = 6.95. In a number of experiments (n = 11) the pipette was filled with salines where the pH of the pipette solution was 6.05. We were never able to observe channel activity under these conditions.

Detached patch, conductance ratios, and selectivity

In the detached mode solutions of varied composition can be perfused onto one side of the patch. Typically the pipette contained either CsCl or KCl saline. Fig. 4 shows tracings of channel activity in the detached mode from various experiments in different perfusates. In all, six conditions are illustrated from six different experiments. In four cases shown the pipette was filled with KCl saline and the bath contained either K^+ (K/K, [Fig. 4 *a*]), Cs^+ (K/Cs, [Fig. 4 *b*]), Na^+ (K/Na, [Fig. 4 *c*]), or tetramethylammonium (K/TMA, [Fig 4 *e*]). In two cases the pipette contained Cs^+ (Cs/Cs, [Fig. 4 *d*], Cs/TEA, [Fig. 4 *f*]). The bath in these two cases contained CsCl saline and TEACl saline, respectively. The pH ranged from 6.6 to 6.8. Table 2 summarizes the equilibrium potentials for each condition and the reversal potentials as determined by *I-V* relationships under each condition. The conductance ratios were calculated with Eqs. 2, 3, and 5.

FIGURE 1 (*a*) The fluorescent probe carboxyfluorescein (CFL) was injected into one of the axonal segments of the median giant axon. The light micrograph shows the outline of the nerve cord and the fluorescence of CFL within the injected cell. The septal membranes are diffusion barriers to the probe, allowing them to be delineated. The horizontal bar in the lower right equals 100 μm. (*b*) The light micrograph of a dissected preparation shows the septal membrane of a median axon protruding from the cut end of the cord. The horizontal bar = 100 μm. A dye filled microelectrode can be seen on the right. (*c*) The fluorescent image of the axon in *b*. The arrow indicates the position of the adjacent septal membrane, the horizontal bar = 100 μm.

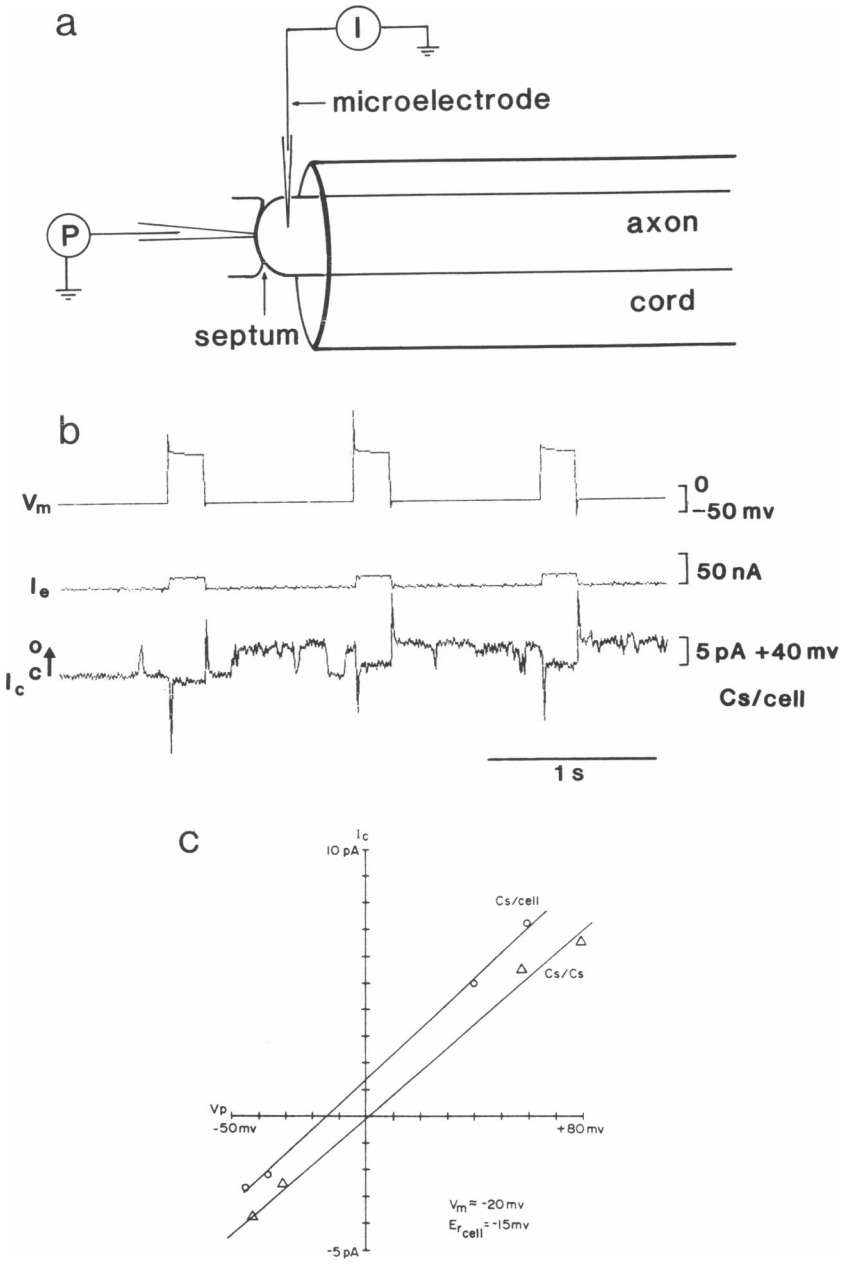

FIGURE 2 The recording setup with attached patch and intracellular electrode is depicted in Fig. 2 *a*. Current pulses were delivered via the intracellular electrode while the patch was held at a specific holding potential. Three tracings are shown in *b*. The trace labeled V_m is the voltage recording from the microelectrode that had been inserted into the intact cell in a preparation like the one shown in Fig. 1. No attempt was made to adjust the pulse artifact with the bridge of the amplifier. The resting potential of the cell was −20 mV. The trace labeled I_e indicates the current being passed via the microelectrode. The trace labeled I_c is the current passing through the septum (attached) patch. The arrow indicates the direction of outward current flow from the patch electrode. The *C* and *O* indicate closed and open states, respectively. Note that with no channel activity the current step from the microelectrode caused little or no deflection of the current from the on-cell patch. During activity (channel open) the current step results in a reduction in the current flow through the channel in the patch. The current step, delivered by the microelectrode, caused a depolarization of the intact cell. The patch was held at +40 mV. The depolarization reduced the voltage across the patch resulting in a reduction in current flow through the channel. The patch electrode was filled with CsCl saline. *c* shows the *I-V* curve for the channel shown while attached (Cs/cell) and after the patch had been detached (Cs/Cs). The unitary current was plotted vs. the holding potential of the pipette. In the detached mode the solutions on either side of the patch were the same. Horizontal bar: 1 s, vertical bar: 5 pA.

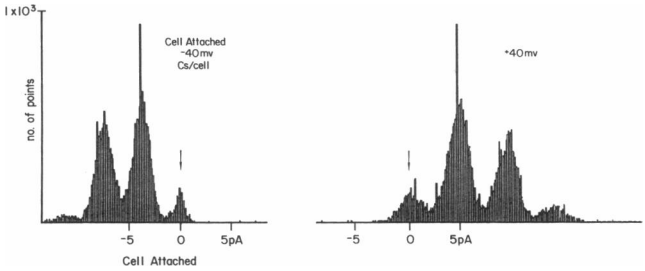

FIGURE 3 Amplitude histograms of current distribution generated (point to point) from channel activity in the attached patch mode are illustrated. The ground state was arbitrarily set to zero. The arrows indicate the zero current point. Data taken from two potentials is shown. When the holding potential was −40 mV there was inward current flow to the pipette representing a negative current. The opposite is true for the +40 mV case. The pipette contained CsCl saline, pH = 6.95. Note that the profiles of the two histograms are mirror images of each other, an expected result if there is no voltage dependence. The data presented here are from a different experiment than that of Fig. 2.

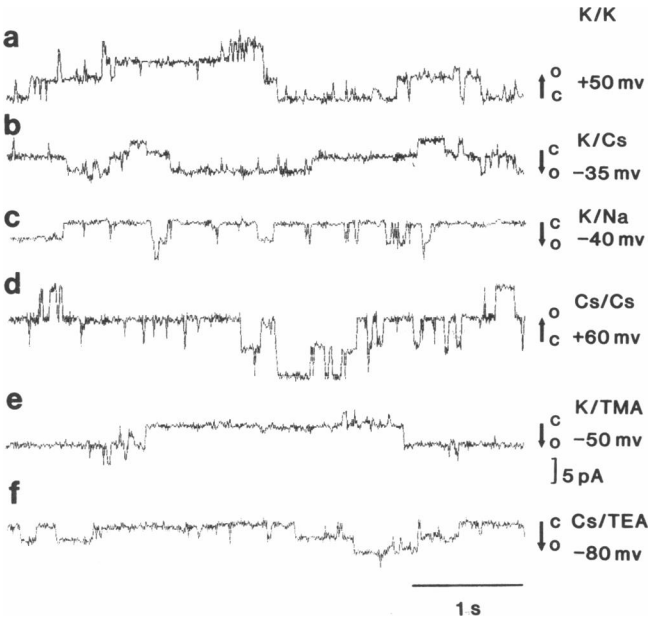

FIGURE 4 Patch recordings in the detached mode under a number of recording and ionic conditions are shown. All the recordings were done with bath and pipette at the same pH but each tracing comes from a different experiment. The first trace *a* is under ionic conditions with KCl on both sides of the patch (K/K) at a holding potential of +50 mV. In the next *b* the pipette contained K^+ while the bath contained Cs^+ (K/Cs). The holding potential was −35 mV. In the third trace *c* the pipette contained K^+ and the bath contained Na^+ (K/Na). The holding potential was −40 mV. In the fourth trace *d* the pipette contained Cs as did the bath (Cs/Cs). The holding potential was +60 mV. In the fifth trace *e* the pipette contained K while the bath contained TMA^+ (K/TMA). The holding potential was −50 mV. *f* illustrates the case where the pipette contained Cs^+ and the bath TEA^+. The holding potential was −80 mV. Data like these were used to determine the reversal potentials listed in Table 2. Arrows indicate the direction of current flow at the patch pipette. Upwards pointing arrows are outward current, downwards inward current flow. *C* and *O* indicate closed and open states, respectively. Horizontal bar: 1 s, vertical bar: 5 pA.

From Ohm's law:

$$I_c = G_K(E - E_K) + G_{Cl}(E - E_{Cl}) \quad (1)$$

when $E = E_r$, $I_c = 0$ thus,

$$G_{Cl}/G_K = [-(E_r - E_K)]/(E_r - E_{Cl}) \quad \text{or,} \quad (2)$$

$$G_{Cl}/G_{Cs} = [-(E_r - E_{Cs})]/(E_r - E_{Cl}). \quad (3)$$

For the other ions the following was used: Again from Ohm's law:

$$I_c = G_K(E - E_K) + G_{Cl}(E - E_{Cl}) + G_x(E - E_x) \quad (4)$$

when $E = E_r$, $I_c = 0$ thus,

$$G_X/G_K = -\{(E_r - E_K) + [(G_{Cl}/G_K)^*(E_r - E_{Cl})]\}/(E_r - E_X), \quad (5)$$

where E_r = reversal potential, all other E values are the equilibrium potentials of the respective ions.

The conductance ratios of the channel followed the sequence: $K^+ = Cs^+ > Na^+ > TMA^+ > Cl^- > TEA^+$ (1.0:1.0:0.84:0.64:0.52:0.20), indicating poor selectivity. The conductance ratio for Cl^- relative to K^+ or Cs^+ was determined by perfusion of the bath with lower concentrations of KCl (55 mM, KCl_{low}) or CsCl (30 mM, $CsCl_{low}$). This experimental procedure set up equal but opposite cation and anion equilibrium potentials. In each case records were first obtained with all ionic conditions equal on either side of the patch, then the KCl_{low} or $CsCl_{low}$ solution was perfused with KCl or CsCl salines in the patch pipette. The G_{Cl}/G_K ratio with either K^+ or Cs^+ (G_{Cl}/G_{Cs}) as the principle cation was 0.52 to 0.57. This was followed by perfusion with KCl or CsCl salines and the reversal potential returned to 0. The data indicate that the observed channel is permeable to both cations and anions. With the exception of Cl^- the selectivity sequence is much like the mobility of the free ions in solution.

Ca^{2+} effects

The effects of Ca^{2+} are shown in Fig. 5. There are four recordings shown where the major cations were K^+ and Cs^+ (K/Cs). The records were obtained in the detached mode. In Fig. 5 *a* the control, the free Ca^{2+} concentration was 10 nM. The second recording (Fig. 5 *b*) shows channel activity within 30 s after perfusion with CsCl saline which contained 2 mM Ca^{2+}; the second record of Fig. 5 *b* was made 2 min after perfusion. The addition of Ca^{2+} to

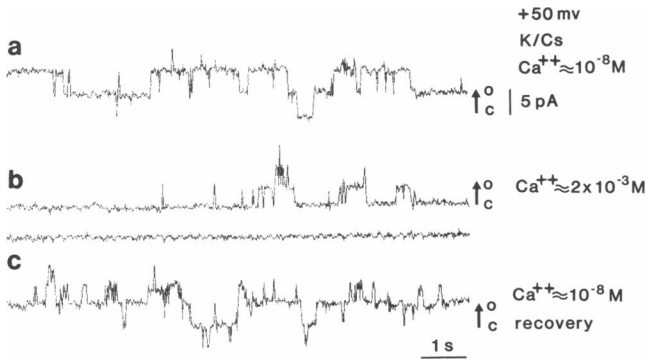

FIGURE 5 The effects of the application of 2 mM Ca^{2+} (Cs-Ca saline) onto the bath side of a detached patch are shown. The effects were reversible. The holding potential was +50 mV. The first tracing *a* shows control behavior where the free Ca^{2+} is concentration 10 nM. Application of 2 mM Ca^{2+} to the bath reduced channel activity. The two center tracings *b* show activity 30 s and 2 min (bottom trace of the two central tracings) after termination of perfusion with Cs-Ca saline. The trace labeled *c* was obtained after reperfusion with CsCl saline (10 nM Ca^{2+}) for 3 min. The pH was held constant at 6.6 throughout the experiment. Histograms of the data shown here are illustrated in Fig. 6. Arrows indicate the direction of current flow at the patch pipette. *C* and *O* indicator closed and open states. Horizontal bar: 1 s, vertical bar: 5 pA.

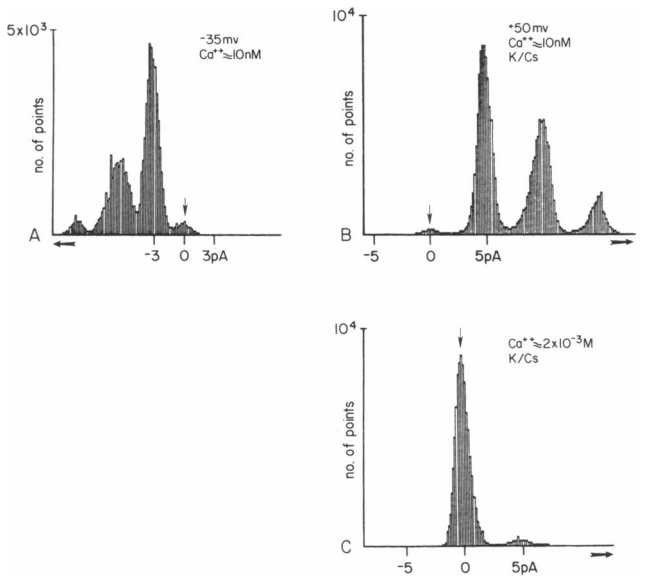

FIGURE 6 Amplitude histograms of current distribution generated from data illustrated in Fig. 5 are shown. Again the lack of effect of holding potential is apparent. *A* and *B* are histograms from the detached patch at −35 mV and +50 mV, respectively. The effect of 2 mM Ca^{2+} is illustrated in *C*. The channel activity is greatly reduced. In *A* the total sample time was 140 s while in *B* and *C* it was 280 s. Vertical arrows indicate the zero current point while the horizontal arrows indicate the direction of current flow, to the right, outward current and to the left, inward current relative to the pipette.

the bath greatly reduced the open time of the 90–110 pS channel. Reperfusion with CsCl saline at a low Ca^{2+} concentration (pCa = 8) resulted in recovery of activity as indicated in Fig. 5 *c*. The holding potential in all cases shown in Fig. 5 was +50 mV. The Ca^{2+} concentration in the pipette was 10 nM and the pH of the bath and pipette was 6.6 throughout the experiment. Fig. 6 (*B*, *C*) illustrates amplitude histograms of current distribution for the data illustrated in Fig. 5. A (holding potential = −35 mV) and Fig. 6 *B* (holding potential = +50 mV) show that in detached modes the unitary or channel activity is voltage independent, as has been illustrated for attached patch (Fig. 3). Fig. 6 *C* (holding potential = +50 mV) is the histogram of current distribution with 2 mM Ca^{2+} on one side of the detached patch. Channel activity was greatly reduced. The number of unitary (channel) events in Fig. 6 *A* was 345, in Fig. 6 *B* there were 957 events and Fig. 6 *C* the number of events was 79. Sample duration was 140s in Fig. 6 *A* and 280s in *B* and *C*.

H^+ effects

The effects of elevated H^+ are shown in Fig. 7. The trace in (Fig. 7 *a*) demonstrated control conditions (Cs/Cs, pH = 6.9). Perfusion with pH = 6.05 Cs saline (Fig. 7 *b*) caused a reduction in channel activity. Recovery of channel activity with pH = 6.9 saline is shown in (Fig. 7 *c*). We found that channel activity could be readily observed

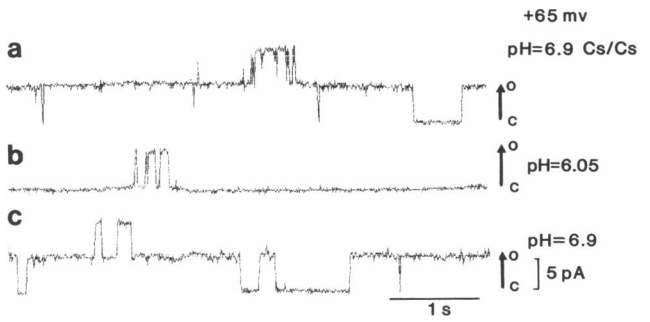

FIGURE 7 The effects of elevated H^+ in the bath are shown. The effects of H^+ were reversible. Trace *a* shows channel activity of a detached patch at pH = 6.9 with Cs on either side of the patch. The holding potential throughout was +65 mV. At least two channels are active in the patch. Trace *b* shows the effects of pH = 6.05 in the bath. The record was obtained 1 min after the termination of a 1 min perfusion with the pH = 6.05 CsCl saline. Trace *c* was taken after reperfusion (2 min) with pH = 6.9, CsCl saline. Channel activity recovered. Arrows indicate the direction of current flow (outward) from closed (*C*) to open (*O*). Horizontal bar: 1 s, vertical bar: 5 pA.

between pH = 6.4 and 7.5 but below 6.4 activity was greatly reduced. The pH of the pipette solution was pH = 6.9 throughout the experiment. At least two channels with the same unitary current can be seen in the records. Fig. 8 shows the histograms for the data illustrated in Fig. 7. The arrow in the four panels indicates the ground state which was arbitrarily set to zero. The four panels illustrate the effects of pH on total open time probability for the two levels shown. The total number of events in Fig. 8 *A* was 381 while in Fig. 8 *B* it was 191, and in Fig. 8 *C* and *D* they were 35 and 296, respectively. All sample durations was 140 s. In Fig. 8 *A* the pH was 6.95. Perfusion with CsCl saline in pH = 6.4 reduced activity such that the double open state (two open channels) disappeared leaving only the first or single open level. In Fig. 8 *C* the patch was perfused with pH = 6.05. Almost all activity is eliminated. Reperfusion with CsCl saline of pH = 6.95 resulted in recovery of channel activity. The fact that one open level was relatively unaffected by pH = 6.4 while the other was eliminated imply that the two open levels (channels) have varied pH sensitivities or different pKs. In Fig. 8 *D* pH = 6.95 produced recovery that was not complete but two open levels can again be observed. The holding potential throughout was +65 mV. Macroscopic measurements of septal membrane junctional conductance indicate that acidification of the cytoplasm followed by realkalinization results in only partial recovery relative to control conductance (Brink et al., 1988*a*).

Voltage independence

Figs. 3 and 6 have already illustrated that channel activity is apparently unaltered by voltage. Voltage independence is again illustrated in Fig. 9. The pipette solution was CsCl saline and the bathing solution was identical; pH was 6.9 in both solutions. The records shown in Fig. 9 are from a detached patch. In addition, in this particular experiment 4 mM 4-aminopyridine was added to both solutions. Amplitide histograms at four different holding potentials ranging from −90 mV to +50 mV are illustrated in Fig. 9 *A–D*. At all four potentials at least two channels are active. The histograms could not be fit using a single probability regardless of the number of channels, at the very least two probabilities would be required (R. Mathias and S. V. Ramanan, personal communication). In histogram *A* (Fig. 9) the total number of unitary events was 263; in *B* it was 190; in *C* 209, and in *D* it was 251. The botton panel in Fig. 9 illustrates recordings from the data set used to generate the amplitude histograms. The arrows in all four cases indicate the closed state.

Comparisons of the amplitude histograms of Figs. 3, 6, and 9 with those obtained from double whole cell patch

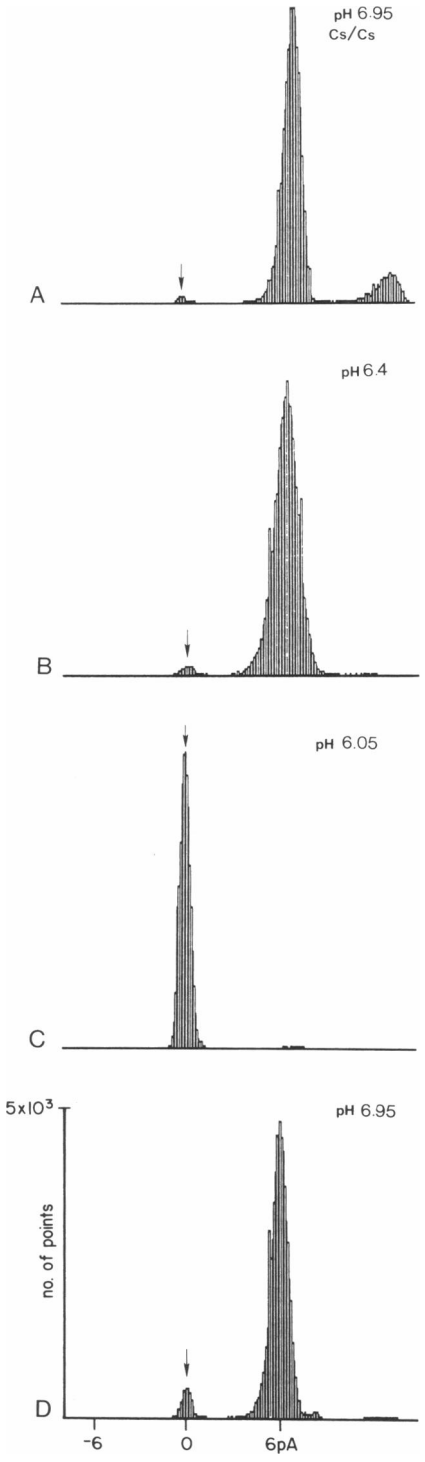

FIGURE 8 Histograms from data illustrated in Fig. 7 are shown. In each case (*A–D*) 140 s of data were analyzed. The holding potential was +65 mV. In *A* the pH was 6.95 in *B* it was 6.4, in *C* it was 6.05, and in *D* (recovery) it was 6.95. The vertical arrows indicate the zero current point. The second open level appears to be more pH sensitive than the first.

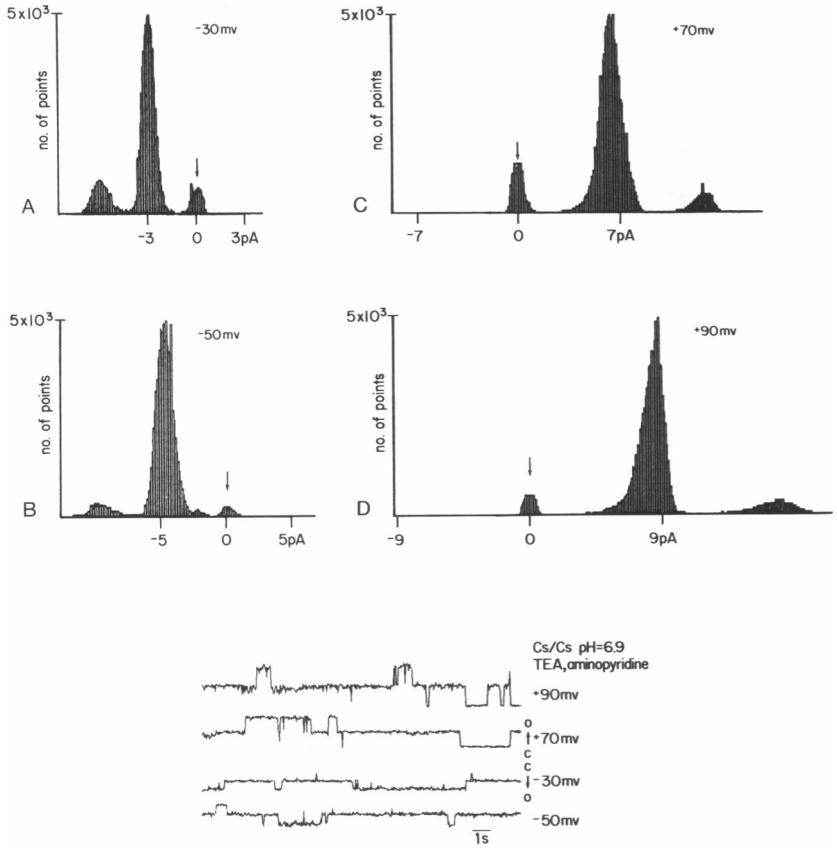

FIGURE 9 *A–D* are histograms derived from data illustrated in the lower panel. In each case sample duration was 140 s. The holding potentials were +90, +70, −30, and −50 mV. The vertical arrow indicates the closed or ground state. The records in the lower panel indicate that there are at least two channels in the patch. These recordings are from a detached patch where both the pipette and bath contained CsCl saline at pH = 6.9. In addition 4-aminopyridine was present in pipette and bath.

records of pancreatic acinar cell pairs and hamster ovary cells illustrated in Somogyi and Kolb (1988) is startling. The amplitude histograms show a very similar kind of behavior to that illustrated in Figs. 3, 6, and 9. To further illustrate the voltage independent behavior of these channels a histogram of number of events per minute vs. potential was constructed (Fig. 10 *a*). There was no significant change in the number of events at any of the four potentials. For comparison the data for Ca^{2+} and H^+ is also illustrated in the same manor. In both cases the number of events per minute is reduced.

DISCUSSION

The poor selectivity and lack of effect of agents known to reduce the activity of other well documented channels are important elements in discriminating between the 100 pS channel and other channels. Comparison of the conductance ratios with those of other channels of known diameters implies that the 100 pS channel is a large bore channel. Other important criteria are whether Ca^{2+} and H^+ affect channel patency. While no macroscopic data are available with regard to the Ca^{2+} effects on the septal membrane of earthworm, the effect of cytoplasmic acidification has been demonstrated (Verselis and Brink, 1984). Macroscopic measurements under double voltage clamp indicate that the gap junctions of the septal membranes are voltage independent (Brink et al., 1988) therefore the 100 pS channel should also be insensitive to potential whether recording in attached or detached mode.

Selectivity

The lack of selectivity of the 100 pS channel is clearly demonstrated by the comparison of the conductance ratios for Cs^+, Na^+, TMA^+, Cl^-, and TEA^+ relative to K^+ (Table 2). The sequence and ratios given in Table 2 are unlike those found for other channels (Hille, 1984).

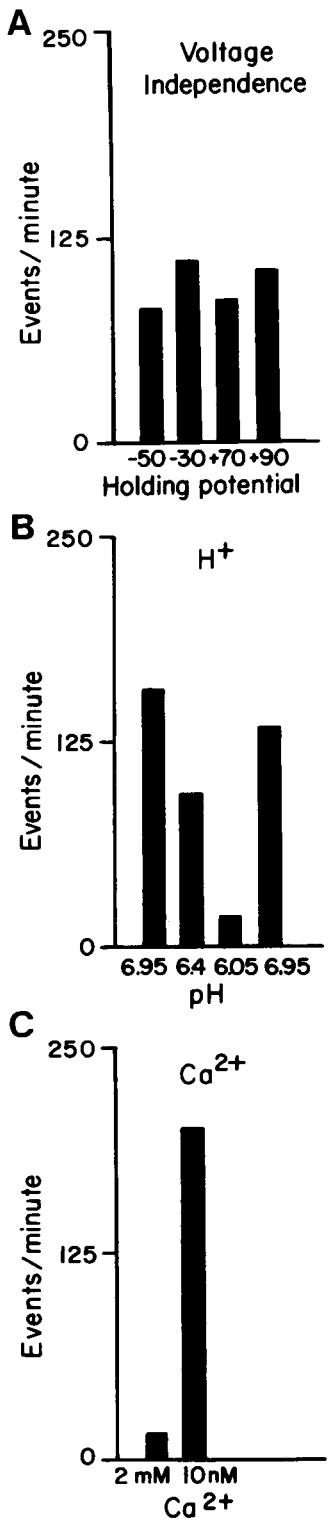

FIGURE 10 *A–C* represent histograms of the number of events/minute (channel openings and closings). In *A* the number of events/minute is plotted vs. holding potential (data from Fig. 9). In *B* the effect of H^+ is illustrated and in *C* the effect of Ca^{2+} is shown. In *B* and *C*, H^+, and Ca^{2+} reduce the number of events/minute.

The only other study where conductance (permeability) ratios were determined for the gap junction was that of Neyton and Trautmann (1985). They found G_{Na}/G_K = 0.81 and G_{Cl}/G_K = 0.67 for the gap junction channel in rat lacrimal gland cell pairs, values similar to those reported here (Table 3).

None of the K^+ channels, including delayed rectifiers, inward rectifiers, Ca^{2+} activated K^+ or light activated K^+ channels, passes Cs^+ or Na^+ (Hille, 1984) with the ease of the channel described here. The same is true for Na channels and endplate channels. Further, the ease with which the 100 pS channel passes TMA^+ and TEA^+ indicates that the channel diameter is probably greater than the dimensions of K^+, Na^+, or endplate channels (Hille, 1971, 1972, 1973; Adams et al., 1980).

Comparison of the selectivity sequence for the 100 pS channel with that of large bore channels such as porin demonstrates that the 100 pS channel is apparently larger in diameter than porin. Porin is a channel forming protein, referred to as OmpF (37 Kd) by Benz (1986), found in the membrane of *Escherichia coli* (Benz et al., 1980). Porin (OmpF) from *Escherichia coli* was chosen because it is able to pass both cations and anions. Other porin channels are selective for cations over anions and vise versa (Benz, 1986). The channel diameter of the 37 Kd porin is 0.9 to 1.0 nm and is relatively nonselective with a single channel conductance of 190 pS. The porin channel subunits are thought to form beta sheets (Engle et al., 1985) while connexins have been reported to form beta sheets as well as alpha helical structures (see Paul, 1985). For the porin channel, the conductance ratios relative to K^+ for the same sequence of ions used in this study are 1.0:1.05:0.63:0.35:0.09:0.03 (Cs > K > Na > Cl > TMA > TEA, Table 3, Benz et al., 1980). Conductance increments were measured with equimolar salt on either side of a porin loaded bilayer. Because the permeability ratios for TMA^+/K^+ and TEA^+/Cs^+ are much larger for the 100 pS channel than in the porin channel (0.64 vs. 0.09 for TMA^+ and 0.2 vs. 0.03 for TEA^+), the diameter of the 100 pS channel observed here is presumed to be larger than that of porin. Comparison of the selectivity sequence with that of the maxi-K channel (BK) also demonstrates the same point (Table 3). In case of the maxi-K channel Cl^- can not pass through the channel and TEA blocks the channel rather than being allowed to pass through it (Blatz and Magleby, 1984). Both porin and the maxi-K have larger single channel conductances but are more selective. The larger conductances in these two cases are a function of the length of the two channels, ~ 3.0 and 1.0 nm vs. 15.0 nm for the gap junction channel. However, the selectivity comparisons do not unequivocally demonstrate that the bore of the 100 pS is larger than porin or the maxi-K channel.

TMA^+ in unhydrated form has a diameter of ~ 0.65

TABLE 3 **Channel comparison**

100 pS channel	Porin*	Gap junction channel‡	Maxi-K channel§
K = Cs > Na > TMA > Cl > TEA	Cs > K > Na > Cl > TMA > TEA	K > Na > Cl	K > Cs > Na
1.0:10:0.84:0.64:0.52:0.2	1.05:1.0:2.63:2.35:0.09:0.03	1.0:0.81:0.67	1.0:2.05:0.01

*Benz et al., 1980.
‡Lacrimal gland gap junction, Neyton and Trautmann, 1985.
§Calcium activated maxi-K Channel, Blatz and Magleby, 1984.

nm and TEA^+ has an unhydrated diameter of 0.8 nm. Using radio-labeled TEA^+ and K^+ Weingart (1974) was able to determine the permeability ratio for the two ions in the intercalated disc of ungulate myocardial cells. $P_{TEA}/P_K = 0.13$ in that study, a value similar to that determined for the 100 pS channel. In addition, Verselis et al. (1986, abs) used cation sensitive microelectrodes to show that TMA^+ and TEA^+ can pass through gap junctions of amphibian embryonic cell pairs. It would appear that the 100 pS channel has a diameter comparable to that of the gap junction channel.

Another possible candidate for the identity of the channel observed in the septal membrane is a cation channel, but the passage of an anion would negate this possibility. The analysis yielded a $G_{Cl}/G_K = 0.52$ (Table 2). The channel is able to pass Cl^- but the Cl^- mobility relative to K^+ is reduced in comparison to mobilities in free solution (1:1.02, free solution vs. 1:0.52–0.57, 100 pS channel, 1:0.67 for gap junction channel of lacrimal gland, Neyton and Trautmann, 1985). The G_{Cl}/G_K ratio for the porin channel is 0.35 as opposed to 0.52 for the 100 pS channel. The porin and 100 pS channel appear to show some selectivity for cations over anions. Benz et al., (1980) showed that the cation selectivity of porin was pH dependent such that under acid conditions (pH = 2) cation selectivity was nonexistent relative to anions. They concluded that the cation-to-anion selectivity was the result of the presence of fixed negative charges within the pore. The gap junction channel and the one observed here are sensitive to pH (Spray et al., 1982; Turin and Warner, 1980). The probability of opening for the 100 pS channel is greatly reduced at acidic pH, making it impossible to replicate the experiment of Benz et al. (1980). Based on previous studies with fluorescent probes, the presence of a fixed anionic site(s) in the gap junction channel has been proposed (Flagg-Newton et al., 1979; Brink and Dewey, 1980), a conclusion that is consistent with the findings presented here.

Suppressive effects of Ca^{2+} and H^+

Ca^{2+} and elevated H^+ reduce junctional membrane conductance or permeability (Loewenstein, 1981; Spray et al., 1984; Spray and Bennett, 1985). More recently, Girsch and Peracchia, (1985; see also Peracchia, 1987) have shown that calmodulin is necessary to impart Ca^{2+} sensitivity to reconstituted lens MIP26 in liposomes. A free Ca^{2+} concentration of 100 μM was able to reduce liposome swelling with calmodulin, but without calmodulin Ca^{2+} had no effect. The concentration of Ca^{2+} required to uncouple intact cells has been reported to be much lower than 100 μM. Loewenstein (1981; see also Noma and Tsuboi, 1987) has demonstrated that Ca^{2+} levels as low as 1 μM are effective in reducing junctional membrane conductance. Spray et al. (1982) reported that Ca^{2+} concentrations of 1 mM were required to occlude gap junction channels. In their experiment one cell of a pair fundulus embryonic cells was cut open to allow access of a perfusion electrode. It might well be that the variability in Ca^{2+} sensitivities reported is a reflection of the presence or state of calmodulin or calmodulin-like substances (cytoplasmic intermediates, Peracchia, 1987) in the vicinity of gap junction channels. The data shown in Fig. 6 *C* indicate that the probability of opening of the 100 pS channel is greatly reduced by 2 mM Ca^{2+}. It appears that Ca^{2+} alters open time via gating or by blocking the channel orifice. We have not yet determined the lower limit of the 100 pS channels sensitivity to Ca^{2+}.

Elevated H^+ also reduced the total open time probability (Figs. 7 and 8). The data shown in Fig. 8 also indicate that at least two different types of gap junction channels exist with regard to pH sensitivity. It is impossible to determine from these data whether Ca^{2+} and H^+ are acting on the same gate(s) or not.

Lack of voltage dependence

Voltage dependence is not clearly demonstrable with the 100 pS channel (Fig. 9). It seems unlikely that the records contain K^+ or other channels simply because of the agents present that are known to block or reduce the activity of other channels (Cs^+, TEA^+, Zn^{2+}, Co^{2+}, and Ni^{2+}). The histograms shown in Figs. 3, 6, and 9 indicate that total open time probability is not altered by varying voltage. It would appear that the histograms can not be fit by a multinomial distribution using a single opening probabili-

ty; (R. Mathias and S. V. Ramanan, personal communcation). It is conceivable that the histogram activity results from a cooperative behavior of channels all with the same independent probability of opening, this however remains to be determined.

The number of channels predicted to be within the pipette is important to the analysis presented. Brink and Dewey (1980) calculated the number of gap junction particles per square micron on the septum to be 290. Assuming an even distribution of particles, channel activity should be present in almost every patch. In fact only one in eight showed channel activity on average. Electron micrographs of the septal membrane reveal small loosely arranged aggregates of gap junction particles (Kensler et al., 1979; Brink and Dewey, 1980) such that the patch pipette tip could contain from many (hundreds) to few or no gap junction channels. Here we only recorded from patches with apparent seals of 2 GΩ or better. Thus patches which could potentially contain many active channels which presumably had significantly high open time probabilities (10%) would have yielded apparent seal resistances <1 GΩ. The morphology (Kensler et al., 1979) is consistent with patches that contain only a few channels but predict patches that contain many channels that we have avoided on the basis of apparent seal resistance. Another possibility might be that many of the gap junction channels under normal physiological conditions are not active or have very low open time probabilities. The rigors of the dissection and solution exposure could also render many channels inactive.

The question of how Co^{2+} and the other substances used to block other channel activity might affect gap junction channel patency is difficult to address directly. Clearly these agents are tolerated by the 100 pS in the sense that the channel can open and close when they are present. Co^{2+} has been shown to pass through junctional membranes but only when the cytoplasmic concentration is low (Politoff et al., 1974). Whether or not any of the other agents enlisted for this study affect gating is a question that requires further study.

Gap junction channel or hemichannel?

The hemichannel is half the length of the intact gap junction channel. The conductance of the hemichannel should be approximately double that of a gap junction channel. Using Ohm's law the predicted conductance of a channel with a length of 15 nm and diameter of 1.5 nm with a bathing media resistance of 80 Ω-cm (135 mM KCl saline) is 147 pS. This value represents the upper limit expected for the single channel conductance of the gap junction. Typically channels possess conductances that are less than the limit predicted by Ohm's law (Hille, 1984). For the hemichannel with a length of 7.5 nm and the same presumed diameter the optimal conductance would be 293 pS. Thus the hemichannel conductance should be in the range of 200 pS as opposed to the observed value of 100 pS. This argument is not conclusive but is consistent with the notion that the 100 pS channel is an intact gap junction channel. For comparison the porin channel has a single channel conductance of ~190 pS under ionic conditions similar to those used here and the limiting conductance derived from Ohm's law is 240 pS. Channel diameter is assumed to be 0.9 nm and length 3.0 nm, (Benz et al., 1981). A similar argument can be made for the maxi-K channel. With a channel length of 1 nm and diameter of 0.6 nm the limiting conductance would be 350 pS vs. the observed 230 pS (Blatz and Magleby, 1984). Note also in those experiments where gap junction subunits were incorporated into bilayers conductances of 140–270 pS were observed (Ding-E Young et al., 1987; Hall and Zampiphi, 1985). It is easier to imagine the subunits forming a hemichannel rather than an intact 12 subunit channel. When whole gap junction membrane fragments (double membrane) were incorporated into bilayers a single channel conductance of 150 pS was observed (Spray et al., 1986). Again these data are consistent with the notion that the single channel conductance of a hemichannel should be higher than 100 pS.

CONCLUSIONS

The data presented illustrate a 90–110 pS channel, which allows the passage of cations in a sequence that approximates the ionic mobilities of those same cations in free solution. In addition, the channel is only poorly selective for cations relative to anions ($G_{Cl}/G_K = 0.52$). The channel appears to be unaffected by K^+ channel blockers such as Cs^+ and TEA^+; in fact Cs^+ passes as readily as K^+. Other channel blockers such as Ni^{2+}, Co^{2+}, and Zn^{2+} are also unable to alter the patency of the 100 pS channel. The channel(s) show little or no voltage sensitivity in both attached and detached modes. The 100 pS channel is also in electrical contact with the intact cell as shown by attached mode recordings. Further, probability of opening is reduced by either Ca^{2+} or H^+. Thus the 100 pS channel has many of the properties expected of a gap junction channel.

The authors would like to thank Dr. L. Barr for insight and encouragement as well as Dr. Mathias and S. V. Ramanan for their insightful analysis of the data. We thank I. Cohn for reading of the manuscript. Thanks also to L. Betti and J. Kelly for technical assistance.

This work was supported by National Institutes of Health grants GM24905 and HL31299.

Received for publication 13 February 1989 and in final form 18 May 1989.

REFERENCES

Adams, D. J., T. M. Dwyer, and B. Hille, 1980. The permeability of endplate channels to monovalent and divalent metal cations. *J. Gen. Physiol.* 75:493–510.

Benz, R., K. Kanko, and P. Langer. 1980. Pore formation by the matrix protein (Porin) of *Escherichia coli* in planar bilayers membranes. *Ann. N.Y. Acad. Sci.* 258:13–24.

Benz, R., 1986 Analysis and chemical modification of bacterial porins. *In* Ion Channel Reconstitution. C. Miller, editor. Plenum Publishing Corp., New York.

Bezanilla, F. 1987. Single sodium channels from the squid giant axon. *Biophys. J.* 52:1087–1090.

Blatz, A. L., and K. L. Magleby. 1984. Ion conductance and selectivity of single calcium-activated potassium channels in cultured rat muscle. *J. Gen. Physiol.* 84:1–23.

Brink, P. R., and M. M. Dewey. 1980. Evidence for fixed charge in the nexus. *Nature (Lond.)* 285:101–102.

Brink, P. R., and L. Barr. 1977. The resistance of the septum of the median giant axon of earthworm. *J. Gen Physiol.* 69:517–536.

Brink, P. R., and M. M. Dewey. 1978. Nexal membrane permeability anions. *J. Gen. Physiol.* 72:69–78.

Brink, P. R., and S. V. Ramanan. 1985. A diffusion model for the septate axon: junctional permeability and cytoplasmic diffusion coefficients. *Biophys. J.* 48:299–309.

Brink, P. R., R. T. Mathias, S. W. Jaslove, and G. J. Baldo. 1988. Steady-state current flow through gap junctions: effects on intracellular ion concentration and fluid movement. *Biophys. J.* 53:795–807.

Brink, P. R., S. W. Jaslove, R. T. Mathias, and F. J. Baldo. 1988*a*. Voltage clamp studies of gap junctions. *Mod. Cell Biol.* 7:321–324.

Burt, J. M., and D. C. Spray. 1988. Single channel events and gating behavior of the cardiac gap junction channel. *PNAS.* 85:3431–3434.

Ding-E Young, J., Z. A. Cohn, and N. B. Gilula. 1987. Functional assembly of gap junction conductance in lipid bilayers: demonstration that the major 27Kd protein forms the junctional channel. *Cell.* 48:733–743.

Flagg-Newton, J. L., I. Simpson, and W. R. Loewenstein. 1979. Permeability of the cell-to-cell membrane channels in mammalian cell junction. *Science (Wash. DC)* 205:404–407.

Girsch, S. J., and C. Peracchia. 1985. Lens cell-to-cell channel protein. II. Conformational changes in the presence of calmodulin. *J. Membr. Biol.* 83:217–225.

Goodenough, D. 1975. The structure and permeability of isolated hepatocyte gap junctions. *Cold Spring Harbor Symp. Quant. Biol.* 40:37–44.

Hall, J. E., and G. A. Zampighi. 1985. Proteins from purified lens junctions induces channels in planar lipid bilayers. *In* Gap Junctions. M. V. L. Bennett and D. C. Spray, editors. 177–189 pp. Cold Spring Harbor Laboratory.

Hille, B. 1971. The permeability of the sodium channel to metal organic cations in myelinated nerve. *J. Gen. Physiol.* 58:599–619.

Hille, B. 1972. The permeability of the sodium channel to metal organic cations in myelinated nerve. *J. Gen. Physiol.* 59:637–638.

Hille, B. 1973. Potassium channels in myelinated nerve. Selective permeability to small cations. *J. Gen. Physiol.* 61:669–686.

Hille, B. 1984. Ionic Channels in Excitable Membranes. Sinauer Associates Inc., Sunderland, MA. 426 pp.

Kensler R. W., P. R. Brink, and M. M. Dewey. 1979. The septum of the lateral axon of the earthworm: a thin section and freeze fracture study. *J. Neurocyol.* 8:565–590.

Loewenstein, W. R. 1981. Junctional intercellular communication: the cell-to-cell membrane channel. *Physiol. Rev.* 61:829–913.

Loewenstein, W. R. 1985. Regulations of cell-to-cell communication by phosphorylation. *Biochem. Soc. Symp.* 50:43–58.

Makowski, L., D. L. D. Capser, W. C. Phillips, T. S. Baker, and D. A. Goodenough. 1984. Gap Junction structures. VI. Variation and conservation in connexon conformation and packing. *Biophys. J.* 45:208–218.

Nanniga, L. B., and Kemper. 1971. Role of Magnesium and Calcium in the first and second contraction of glycerin extracted muscle fibers. *Biochemistry.* 10:2449–2456.

Neyton, J., and A. Trautmann. 1985. Single-channel currents of an intercellular junction. *Nature (Lond.).* 317:331–335.

Noma, A., and N. Tsuboi. 1987. Dependence of junctional conductance on proton, calcium and magnesium ions in cardiac paired cells of guinea-pig. *J. Physiol. (Lond.).* 382:193–211.

Obaid, A. L., S. J. Socolar, and B. Rose. 1983. Cell-to-cell channels with two independently regulated gates in series: analysis of junctional conductance modulation by membrane potential, calcium, and pH. *J. Membr. Biol.* 73:69–89.

Paul, D. L. 1985. Antibody against liver gap junction 27-kD protein is tissue specific and cross-reacts with a 54-kD protein. *In* Gap Junctions. M. V. L. Bennett and D. C. Spray, editors. 107–122 pp. Cold Spring Harbor Laboratory.

Peracchia, C. 1987. Calmodulin-like proteins and communication junctions. Electrical uncoupling of crayfish septate axons is inhibited by the calmodulin inhibitor W7 and is not affected by cyclic nucleotides. *Pfluegers Arch Eur. J. Physiol.* 408:379–385.

Peracchia, C. 1976. Low-resistance junctions in crayfish. Structural changes with functional uncoupling. *J. Cell Biol.* 70:419–439.

Politoff, A, G. D. Pappas, and M. V. L. Bennett. 1974. Colbalt ions across an electronic synapse if cytoplasmic concentration is low. *Brain Res.* 76:343–346.

Saez, J. C., D. C. Spray, A. C. Nairn, E. L. Hertzberg, P. Greengard, and M. V. L. Bennett. 1986. cAMP increases junctional and stimulates phosphorylation of the 27-kDa principal gap junction polypeptide. *PNAS* 83:2473–2477.

Somogyi, R., and H. R. Kolb. 1988. Cell-to-cell channel conductance during loss of gap junctional coupling in pairs of pancreatic acinar and Chinese hamster ovary cells. *Pflugers Arch. Eur. J. Physiol.* 412:54–65.

Spray, D. C., and M. V. L. Bennett. 1985. Physiology and pharmacology of gap junctions. *Annu. Rev. Physiol.* 47:281–303.

Spray, D. C., J. C. Saez, D. Brosius, M. V. L. Bennett, and E. L. Hertzberg. 1986. Isolated liver gap junctions: gating of transjunctional currents is similar to that in intact pairs of rat hepatocytes. *PNAS* 83:5494–5497.

Spray, D. C., R. L. White, A. Campos DeCarvalho, A. L. Harris, and M. V. L. Bennett. 1984. Gating in gap junction channels. *Biophys. J.* 45:219–230.

Stough, H. 1930. Giant nerve fibers of the earthworm. *J. Comp. Neurol.* 50:217–229.

Turin, L., and A. E. Warner. 1980. Intracellular pH in early *Xenopus* embryos: its effects on current flow between blastomeres. *J. Physiol. (Lond.)* 300:489–504.

Veenstra, R. D., and R. L. DeHaan. 1986. Measurement of single channel currents from cardiac gap junctions. *Science (Wash. DC)*. 233:972–974.

Verselis, V., T. A. Baragiello, D. C. Spray, and M. V. L. Bennett. 1988. Conductance of gap junctions in *Drosophila* salivary glands depends on both transjunctional and inside-outside voltages. *Biophys. J.* 53:52a. (Abstr.)

Verselis, V., and P. R. Brink. 1984. Voltage clamp of the earthworm septum. *Biophys. J.* 45:147–150.

Verselis, V., D. C. Spray, R. L. White, and M. V. L. Bennett. 1986. Comparison of gap junctional conductance permeability ratios among early embryonic cells of frog, fish and squid. *Biophys. J.* 49:203a. (Abstr.)

Weingart, R. 1974. The permeability to TEA ions of the surface membrane and the intercolateral disc of sheep and calf myocardium. *J. Physiol. (Lond.)*. 240:747–762.

Weingart, R. 1986. Electrical properties of the nexal membrane studied in rat ventricular cell pairs. *J. Physiol. (Lond.)*. 370:267–284.

White, R. L., D. C. Spray, A. C. Carvalho, B. A. Whittenberg, and M. V. L. Bennett. 1985. Some electrical and pharmacological properties of gap junctions between isolated rat ventricular myocytes. *Am. J. Physiol.* 249:447–455.